Korea-Australia Rheology Journal
Vol. 21, No. 4, December 2009 pp. 281-288

# The assessment of the performance of drug-eluting stent using computational fluid dynamics

**Taewon Seo[1,*] and Abdul I. Barakat[2]**

[1]*School of Mechanical Engineering, Andong National University, Andong, 760-749, Korea*
[2]*Deptment of Aeronautical and Mechanical Engineering, University of California, Davis, CA, USA*

(Received July 30, 2009; final version received November 4, 2009)

## Abstract

Numerical investigations have been conducted on the assessment of the performance of drug-eluting stent. Computational fluid dynamics is applied to investigate the flow disturbances and drug distributions released from the stent in the immediate vicinity of the given idealized stent in the protrusion into the flow domain. Our simulations have revealed the drug concentration in the flow field due to the presence of a drug-eluting stent within an arterial segment. Wall shear stress increases with Reynolds number for a given stent diameter, while it increases with stent diameter for a given Reynolds number. The drug concentration is dependent on both Reynolds number and stent geometry. In pulsatile flow, the minimum drug concentration in the zone of inter-wire spacing occurs at the maximum acceleration of the inlet flow while the maximum drug concentration gains at the maximum deceleration of the inlet flow. These results provide an understanding of the flow physics in the vicinity of drug-eluting stents and suggest strategies for optimal performance of drug-eluting stent to minimize flow disturbance.

***Keywords*** : drug-eluting Stent, restenosis, wall shear stress, drug concentration

## 1. Introduction

The endovascular stents have reduced restenosis rates to 20~35%, while angioplasty result in restenosis in 30~50% within six months following the initial procedure (Chong & Cheng, 2004a, b; Wentzel *et al.*, 2001). More recently, the development of drug-eluting stents appears to have further reduced the incidence of restenosis (Morice *et al.*, 2002; Moses *et al.*, 2003). Unacceptably high rate of restenosis is mainly due to a small vessel size and stent design, and restenosis is considered as a vascular phenomenon of the biological response to injury. Stent implantation into the arterial segment may cause the damage of the vascular endothelium. The thrombus due to the damage after placement of stent forms at the stent wires as well as on the arterial wall between stent wires. The inflammatory response is characterized by the white blood cell and platelet deposition to repair the damaged vascular walls. The development of the neointimal hyperplasia and the proliferation of the smooth muscle cells occur simultaneously with the inflammatory response. Neointimal formation is known as the main cause of in-stent restenosis and subsequent accumulation of extracellular matrix, collagen and macrophages (Bennett, 2003, Edelman and Rogers 1998; Reger *et al.*, 2001). Several studies have demonstrated that the in-stent restenosis develops neointimal growth in the stented arteries (Garasic *et al.*, 2000; Chong & Cheng, 2004a, b). Thus it is known that the in-stent restenosis is due mainly to neointimal hyperplasia. The neointimal growth is associated with the stent-induced arterial injury caused by the deployment of the stent and expansion of the arterial wall. The relatively high restenosis due to the presence of stents has been brought out the necessity to develop the local drug-eluting stent. The drug-eluting stent has been designed to inhibit the unexpected smooth muscle cell proliferation (Suzuki *et al.*, 2001) as well as neointimal hyperplasia. Sirolimus, which is coated on the stent surface, is known as a potent immunosuppressive and antimitotic drug to inhibit the proliferation of the smooth muscle cell. Thus sirolimus-eluting stent will sustain the suppression of the neointimal proliferation in the site of the injury to the vascular endothelium.

Drug released from stent wire can be driven by both convective and diffusive processes. These transport forces are the primary determinants of drug penetration and distribution in the arterial wall and into the bloodstream.

The influence of the stent geometry under both steady and pulsatile flow conditions has been analyzed by Seo *et al.* (2005) using Computational Fluid Dynamics (CFD). They found that a number of geometric and flow parameters play an important role to determine the flow sepa-

*Corresponding author: dongjin@andong.ac.kr

ration in the presence of a stent within an arterial segement. They also found the wall shear stress is elevated over the stent wires while is considerably lower in between wires due to the flow separation. Berry *et al.* (2000) used a combination of flow visualization experiments and computational fluid dynamics (CFD) to demonstrate that the wires of a stent disturb the flow sufficiently to lead the regions of flow separation and weak recirculation in the regions between the wires. Zunino (2004) applied the numerical simulations to investigate the drug release phenomena from the drug-eluting stent to the arterial wall.

The purpose of the present computational study is to investigate the dynamics of drug transport into the blood through the surface coated on the ideal stents under various flow conditions and stent parameters. Of particular interest is the development of a fundamental understanding of the prevailing drug transport conditions on flow separation zones in the vicinity of a drug-eluting stent with Reynolds numbers, stent diameters, Peclet numbers and pulsatile flow. The deployment of a stent influences the geometric flow boundary conditions due to the protrusion into the flow domain. Thus, this study will provide the optimization of the stent design by analyzing the local distribution of the drug released from the drug-eluting stent.

## 2. Computational Methods

In the CFD simulations, the stent is idealized as a series of rigid circular rings of diameter d that are placed within rigid-walled model arterial segment of uniform diameter D. The computational vessels were created with the idealized stent wires as 3 circular rings of diameter d with 100, 200 and 400 μm and inter-ring spacing w, 400 μm. The diameter of native arterial segment is D, 400 μm, and the lengths of the upstream and downstream of the model stent are 2D, respectively. To examine the impact of expanded stent diameter, the computational geometries were created by the stent-to-vessel ratio (LaDisa *et al.* 2004), (D+d)/D, of 1.10: 1, 1.05:1 and 1.025:1, while for reduced stent diameter the stent-to-vessel ratio are 0.90:1, 0.95:1 and 0.975:1, respectively. A schematic of the simulated model geometries used in this computation are depicted in Fig. 1.

Blood considers as an incompressible Newtonian fluid of density, ρ, 1.06 g/cm$^3$ and dynamic viscosity, μ, 3.5centipoise. The process of drug transport through the blood flow is governed by the convection-diffusion equation. The coupled Navier-Stokes equations with convection-diffusion equation were applied in the blood flow;

$$\nabla \bullet \vec{u} = 0$$

$$\frac{\partial \vec{u}}{\partial t} + (\vec{u} \bullet \nabla)\vec{u} = -\frac{1}{\rho}\nabla p + \nu \nabla^2 \vec{u}$$

where ρ is the fluid density, $\vec{u}$ is the fluid velocity vector,

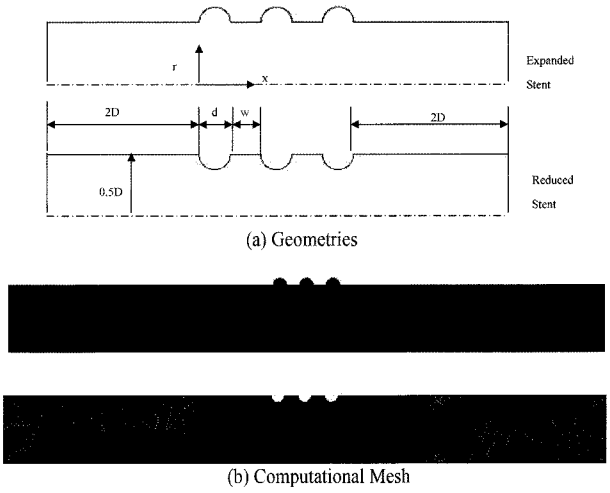


(a) Geometries

(b) Computational Mesh

**Fig. 1.** Idealized geometric stents in either protrusion or dent into the flow domain and meshes.

p is the fluid pressure, and ν is the fluid kinematic viscosity.

The drug transfer into the bloodstream from the drug-coated stent is strongly dependent on convection-diffusion transport. These transport forces can induce the local drug concentration.

$$\frac{\partial C}{\partial t} + (\vec{u} \bullet \nabla)C = \Gamma \nabla^2 \vec{u}$$

where Γ represents the diffusivity, $1.39\times10^{-6}$ cm$^2$/sec, and C drug concentration. All stents were constantly loaded with a fixed amount of drug per unit of metal surface areas (140 μg/cm$^2$).

For the steady flow simulations, the uniform velocity values corresponding to Reynolds numbers are prescribed at the inlet of the arterial vessel.

- Uniform velocity profile; $u = U_{mean} = \frac{\mu Re}{\rho D}$

For the pulsatile flow simulations, the inlet velocity is assumed to be uniform with a non-reversed sinusoidal temporal waveform with a physiological frequency of 1 Hz;

- $u = U_{mean}(1+0.5\sin 2\pi t)$

No-slip velocity conditions are imposed on the arterial wall and the drug elution from the surface of the stent is used as the initial concentration of the drug ($C_{stent}$=140 μg/cm$^2$). At the outlet, flow satisfies zero pressure flow conditions. On the axis of symmetry the axial velocity gradient and cross flow will be zero ($\frac{\partial u}{\partial r} = v = 0$ at r=0). The zero axial concentration gradient was imposed at the outlet ($\frac{\partial C}{\partial x} = 0$ at x=2D) while the zero transverse concentration gradient was applied on the axis of symmetry ($\frac{\partial C}{\partial r} = 0$ at r=0).

All computational domains in this study were composed

of unstructured control volume and simulated symmetric stent and vessel. For all simulations, the meshes ranged from 451,756 to 558,572 triangular cells. The solution of the governing Navier-Stokes equations for the axisymmetric geometries modeled is obtained using commercially available CFD code FLUENT. In FLUENT the momentum is discretized using a first order upwind scheme. The pressure-velocity coupling accomplished through the SIMPLE scheme. In steady flow convergence was based on the residual in continuity and the three velocity components dropping below prescribed values (typically $10^{-6}$ for continuity and the velocity components); this was always achieved within 7000 iterations. In unsteady flow, convergence for each time step was based on the residual in continuity falling below a prescribed value (typically $10^{-6}$). Time-periodic solutions were typically obtained after 4 cycles. All the computations were performed on an Intel Pentium IV 3.20 GHz, 3.50 GB RAM operated Windows XP.

## 3. Results

The drug is eluted in a surface coated on the stent. The drug is transported into the bloodstream by physiological transport forces known as convective and diffusive processes. The spatial and temporal distribution of the drug can be determined by solving the convection-diffusion equations coupled with the Navier-Stokes equations. The numerical method introduced in the previous section is applied to simulate the release of drug into the bloodstream from a drug-eluting stent. The purpose of this study is to investigate the effect of the design parameters of the stent on the drug released process. Therefore, this paper explores the drug concentration in the bloodstream and the possible implication of the efficiency of drug delivery to the vascular wall with different Reynolds numbers, different stent diameters and different diffusivities.

### 3.1. Influence of Reynolds Number

Fig. 2 represents the flow streamlines and drug concentration contours in the blood vessel for three different Reynolds numbers in the case of reduced stent and d/D=0.1. The recirculation flow zone in between stents wires and downstream of the last stent are larger when Reynolds number is higher. Since the drug can reside much longer time in the recirculation zone, it is noted that the drug concentrations downstream in the last stent is more dense in the recirculation regions at lower Reynolds number than at higher one. As Reynolds number increases, the drug downstream in the last stent has be washout due to the strong convective force not to reside in the recirculation zone.

Fig. 3 represents the flow streamlines and drug concentration contours in the blood vessel for three different Reynolds numbers in the case of expanded stent and d/D=0.1.

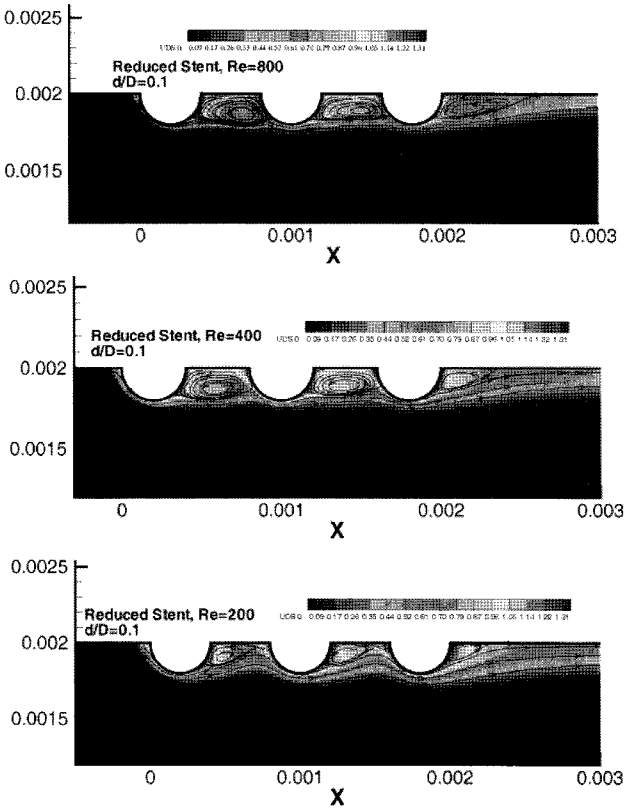


**Fig. 2.** Flow streamlines and drug concentration contours for three different Reynolds numbers in the case of reduced stent and d/D=0.1.

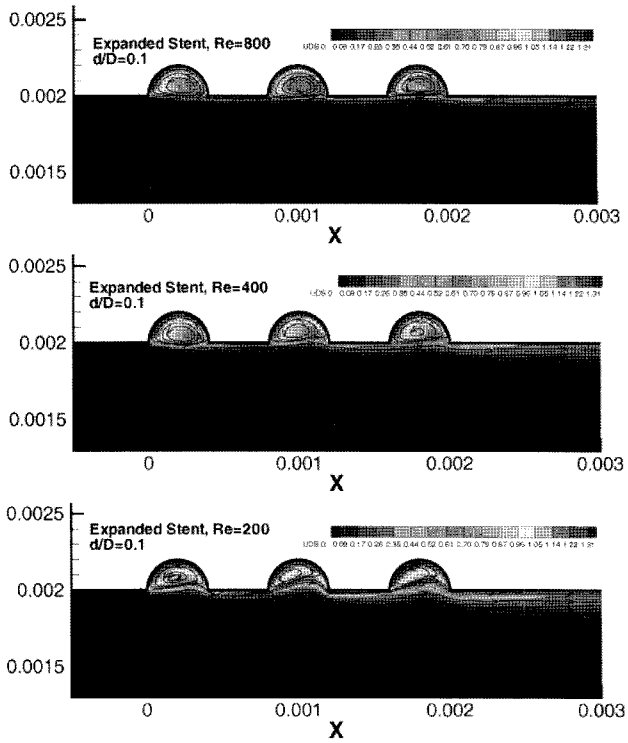


**Fig. 3.** Flow streamlines and drug concentration contours for three different Reynolds numbers in the case of expanded stent and d/D=0.1.

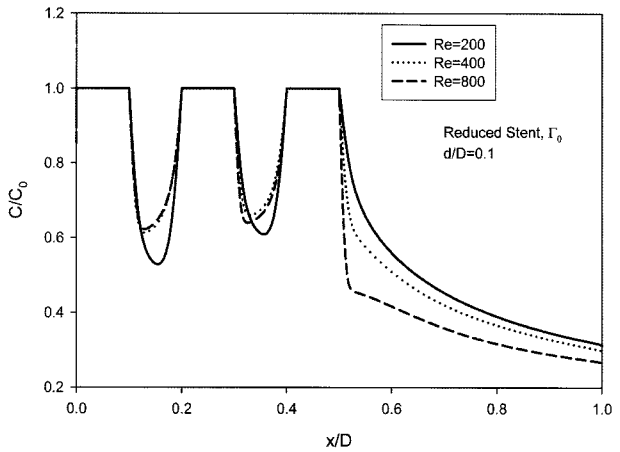


**Fig. 4.** Drug concentration distributions along the arterial wall and stent wires for three different Reynolds number in the case of reduced stent and d/D=0.1.

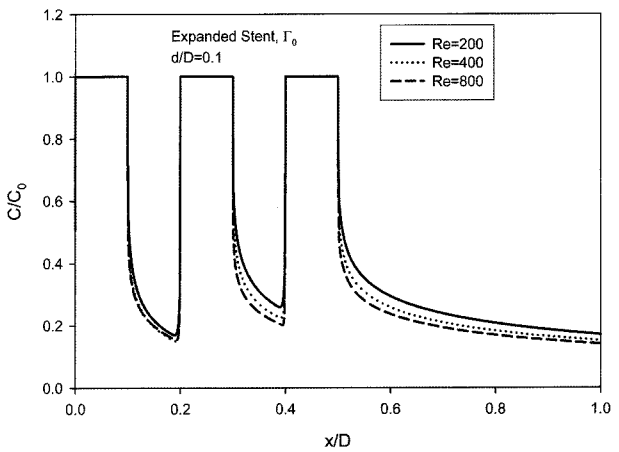


**Fig. 5.** Drug concentration distributions along the arterial wall and stent wires for three different Reynolds number in the case of expanded stent and d/D=0.1.

The large recirculation in the protrusion region of the expanded stent exists when Reynolds number is higher. It is noted that the drug concentration is lower because of the strong convective force for high Reynolds number. As seen in Fig. 3, the blood pushes the flow stream to the stent region when Reynolds number is low. This causes the longer residence in the protrusion region of the drug released from the stent.

Fig. 4 illustrates non-dimensional drug concentration along the arterial walls and stent wires for several Reynolds numbers in the stent-to-vessel ratio is 0.90:1 (Reduced stent) while Fig. 5 represents the stent-to-vessel ratio of 1.10: 1 (Expanded stent). In reduced stent case the drug concentrations in the zone of between stents increase for high Reynolds number and skewed toward the back side of the first and second stents because of the reverse flow due to the front side of the second and third stents. However, it is noted that the drug concentration in the vicinity of the last stent is decreased for higher Reynolds number because of the strong convective momentum to the flow direction.

As seen in Fig. 5, the drug concentration in the case of expanded stent geometry is gradually decreases with increasing Reynolds number. Washout of the drug may minimize the drug concentration for Re=800 even if the recirculation size is larger. As a result, washout of drug strongly depends on the Reynolds number and consequently the drug concentration decreases for higher Reynolds number.

Wall shear stress is calculated in this study as the product of the dynamic viscosity and shear rate of strain. Changes in local vessel geometry after implantation of stent produce the alteration in wall shear stress. Thus we tested the hypothesis that deployment diameter and Reynolds number can affect the wall shear stress.

Fig. 6 represents the results of wall shear stresses in the

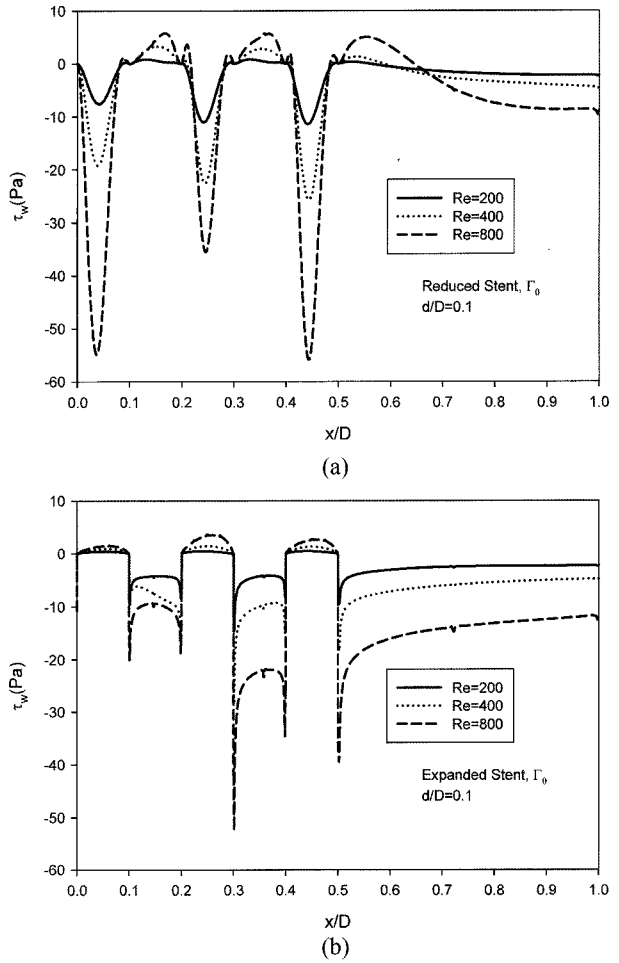


**Fig. 6.** Wall shear stresses in the cases of reduced (a) and expanded (b) stents for d/D=0.1and three different Reynolds numbers.

cases of reduced and expanded stents for d/D=0.1 and three different Reynolds numbers. The stent geometry and Reynolds number have a significantly effect on the dis-

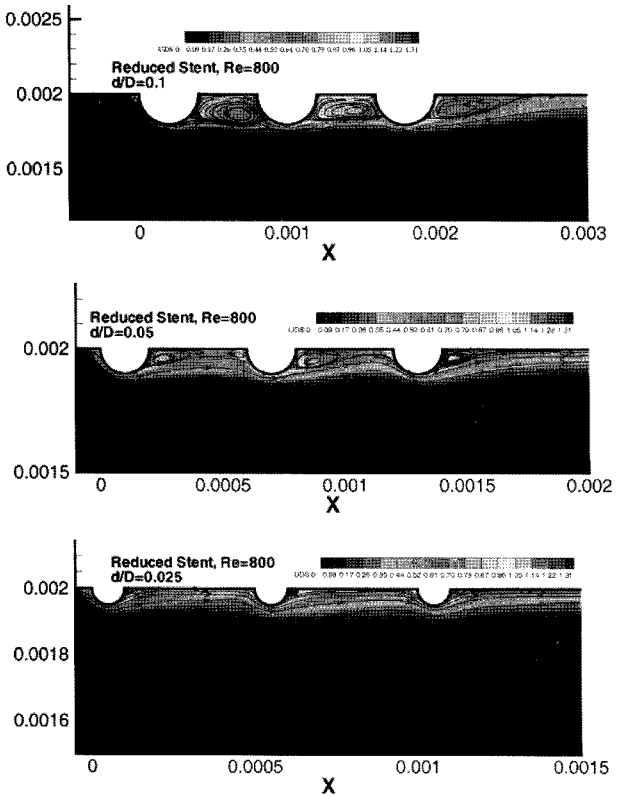


**Fig. 7.** Flow streamlines and drug concentration contours for different stent diameters in the case of reduced stent and Re=800.

tributions of wall shear stress. The highest local wall shear stress magnitude exists over the mid surface of the each stent (see Fig. 6(a). In the expanded stent the recirculation occurs in the protrusion region of the stent, as shown in Fig. 6(b). Regions of low wall shear stress in the case of reduced stent are observed in the recirculation zone depending on Reynolds number. The analytical wall shear stress value of unstented vessel can be determined as

$\tau_{wall} = \frac{8\mu U_{mean}}{D}$. Maximum wall shear stress values between the stents for Re=400 and 800 increase by approximately 20%, but for Re=200 decrease about 30% compared to unstented vessel.

### 3.2. Influence of Stent Diameters

Fig. 7 shows the flow streamlines and drug concentration contours for different stent diameters in the case of reduced stent and Re=800. As expected, the recirculation zone increases when the stent diameter increases. As shown in Fig. 7, the reverse flow occurs in the front of the second stent at d/D=0.05 while it does not occur at d/D=0.025. The drug released along the stent surface is trapped more drug in the region of the recirculation zone increasing the stent diameter, so the drug concentration is high when the stent diameter is large.

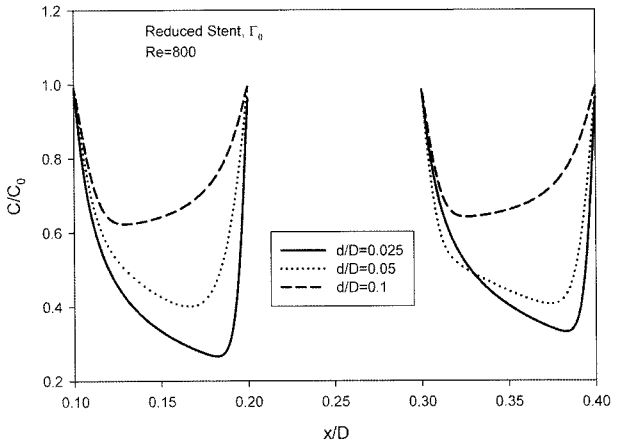


**Fig. 8.** Drug concentration between stents for different stent diameters in the case of reduced stent and Re=800.

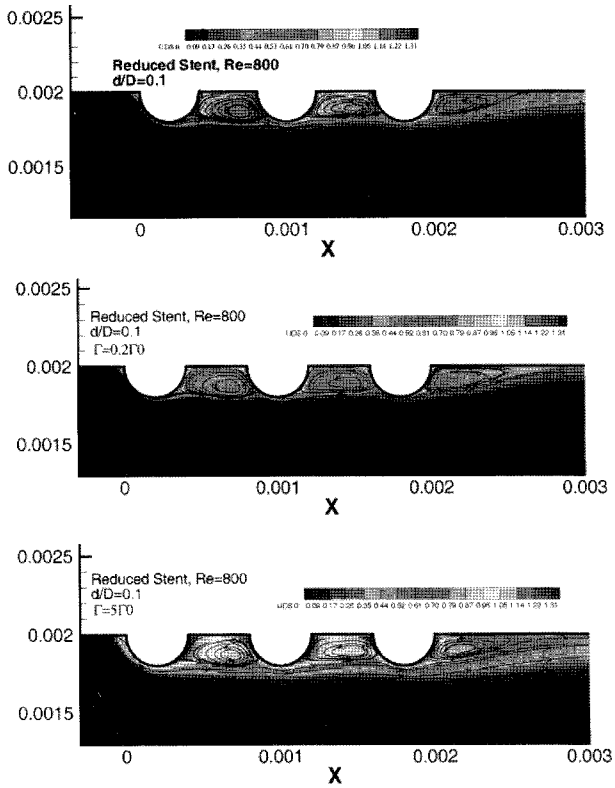


**Fig. 9.** Flow streamlines and drug concentration contours for different diffusivities in the case of reduced stent and Re=800.

Fig. 8 illustrates drug concentration between stents for different stent diameters in the case of reduced stent and Re=800. Since the size of recirculation is larger for large stent diameter than for small stent diameter, and the back flow due to the stent (see Fig. 7), the drug concentration distribution is shifted to upstream increasing Reynolds number. It is noted that the drug concentration is much denser since the reverse flow has strongly affected in the front region of the second and third stents for Re=400 and 800.

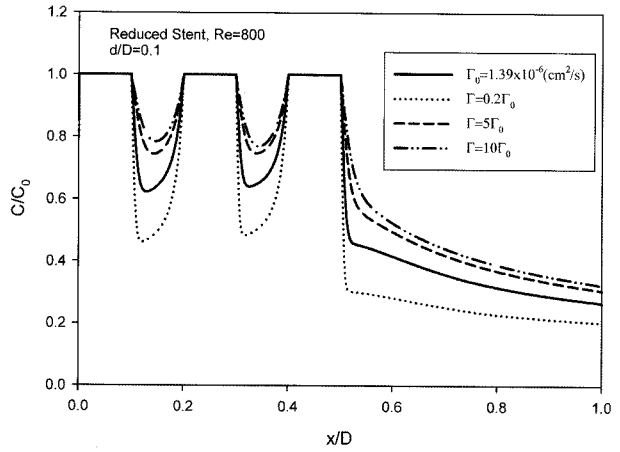


**Fig. 10.** The drug concentration along the arterial wall and stent wires for several different diffusivities in the case of reduced stent and d/D=0.1.

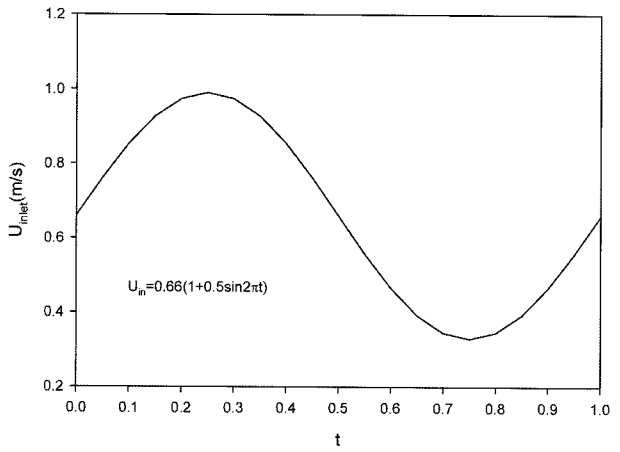


**Fig. 11.** The inlet velocity wave form of a 1-Hz sinusoidal pulsatile cycle.

### 3.3. Influence of Diffusivity

Fig. 9 shows the flow streamlines and drug concentration contours for different diffusivities in the case of reduced stent and Re=800. As shown in governing equations, the drug diffusivity does not affect the flow characteristics. As a result, the flow streamlines are exactly same in Fig. 9. The drug concentration in the regions of between stents is increased when the diffusivity is large (see Fig. 10). If the diffusivity is large under the same Reynolds number and stent geometry, the drug can be diffused denser into the blood stream and trapped much drug in the recirculation zone. The drug distribution in the region between the stents for low diffusivity shift toward the upstream.

### 3.4. Influence of Pulsatile flow

In this section, the results of pulsatile case are presented. Fig. 11 shows the time evolution of the inflow condition during the course of a 1-Hz sinusoidal pulsatile cycle. The mean Reynolds number is 800 and the corresponding

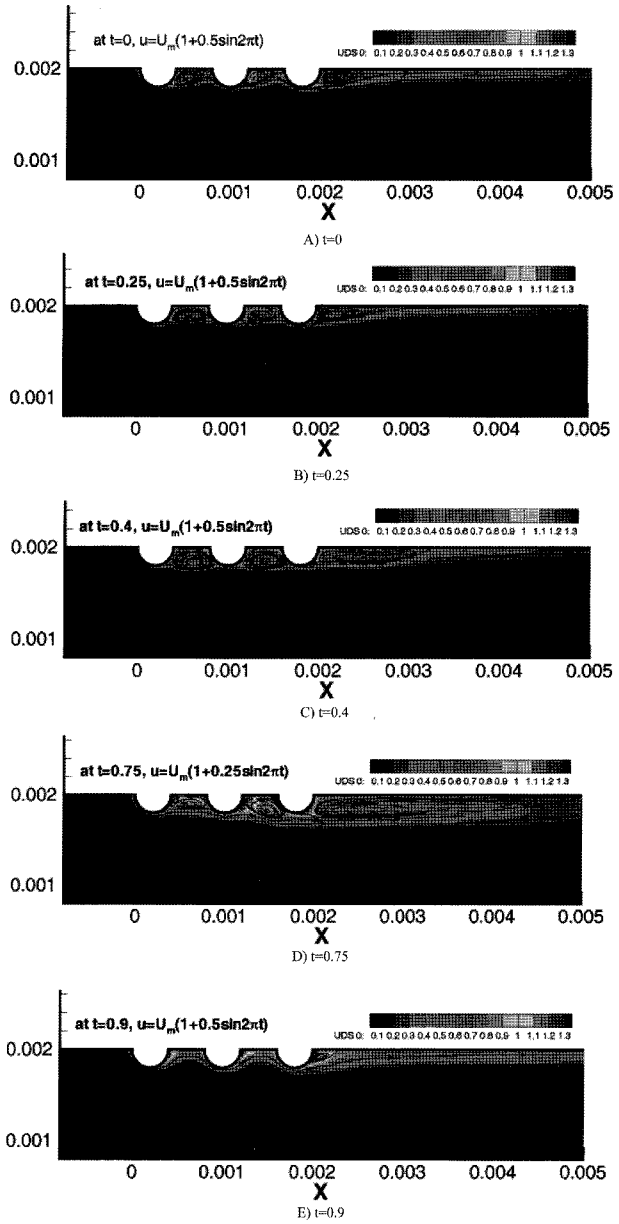


**Fig. 12.** The time evolution of the streamlines and the drug concentration at the five distinct times under the pulsatile inflow condition in the case of the mean Re=800 and d/D=0.1.

Womersley number is 2.76 in this case. Womersley number is defined as $\alpha = \frac{D}{2}\left(\frac{\omega}{\nu}\right)^{\frac{1}{2}}$, where D is the diameter of the vessel, $\omega$ angular frequency of the oscillation and $\nu$ the kinematic viscosity. As shown in Fig. 11, the inflow accelerates early in the inlet velocity temporal waveform and reaches a maximum of 0.99 m/sec at t=0.25. After this point, the velocity magnitude begins to decrease and drops 0.33 m/sec at t=0.75.

Fig. 12 illustrates the time evolution of the streamlines and the drug concentration at the five distinct times under

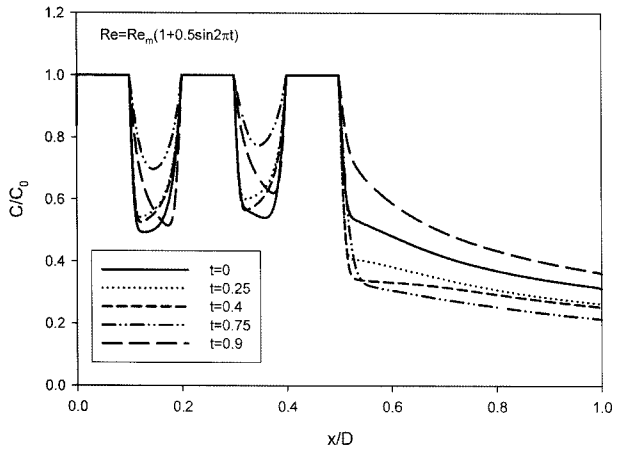


**Fig. 13.** The time evolution of the drug concentrations along the blood vessel and stent walls for five distinct times.

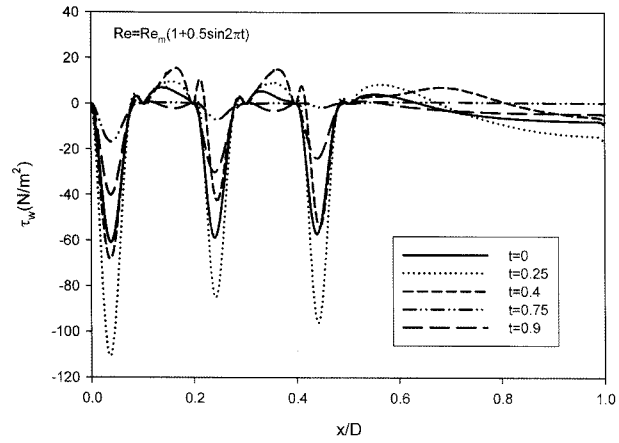


**Fig. 14.** The time evolution of the wall shear stresses along the blood vessel and stent walls for five distinct times.

the pulsatile inflow condition in the case of the mean Re=800 and d/D=0.1. At t=0, when the flow is in acceleration, the flow sees a more favorable pressure gradient, and the separation zones are smaller than the steady flow case (see Fig. 2). However, at t=0.75, the flow is in deceleration, the flow sees a more adverse pressure gradient so that the separation zone is the largest. The drug concentration in the zone of between stents depends on the time varying Reynolds number (see Fig. 13). The minimum drug concentration in the zone of between stents occurs at the maximum acceleration of the inlet flow while the maximum drug concentration gains at the maximum decelerating of the inlet flow. The more drug diffuses downstream of the last stent when the flow is in deceleration because of the larger recirculation region (see Fig. 12 and 13).

Fig. 14 represents the time evolution of the wall shear stresses along the blood vessel and stent walls for five distinct times. Fig. 14 is shown the wall shear stresses have a local maximum values at the middle of the stent depending on the time varying inlet conditions. The minimum wall shear stress in the zone of between stents occurs at the lowest inlet velocity and the wall shear stress increases as the flow accelerates with time. The minimum wall shear stress in the vicinity of the last stent occurred at the lowest inlet velocity condition as shown in Fig. 14. The low and oscillatory wall shear stress distribution imposed on the blood vessel after the placement of the stent may influence the response of intimal hyperplasia. As shown in Fig. 14, regions of low wall shear stress were localized in the zone of between stents due to the flow separation and stagnation flow immediately upstream and downstream of the stents.

## 4. Concluding Remarks

In this study, we have used computational fluid dynamic simulations to investigate the drug concentration in the arterial wall with different Reynolds numbers, stent diameters and diffusivities. Our simulations have demonstrated that the presence of a drug-eluting stent within an arterial segment induces local disturbance in the flow field.

As a result of this flow disturbance, the peak wall shear stress is occurred on the surface of mid stent but is considerably lower in between stents and immediately downstream of the last stent. This leads to large spatial gradients in wall shear stress near the stent. The magnitude of wall shear stress near the stent depends in a complex fashion on the stent geometry and on the flow conditions. For instance, in reduced stent, the wall shear stress depends on both the stent diameter and the flow Reynolds number. For a given stent diameter, the wall shear stress increases with Reynolds number, while for a given Reynolds number, the wall shear stress increases with stent diameter.

The drug concentration is dependent on both the Reynolds number and stent geometry, and resulting effects on the transport of eluted drug. The drug concentration in the zone of between the first and the second stents is lower for the expanded stent because of the existence of more drugs trapped inside of stent zone. Drug concentration decreases along the arterial wall behind the last stent by strong convection increasing Reynolds number.

Although the present results provide some information, the 3-dimensional studies included the complex geometries such as curved vessel need to be considered. In summary, the deployment of stent alters the flow disturbances and the drug distribution. These results provide an understanding of the flow physics in the vicinity of drug-eluting stents and suggest strategies for optimal performance of drug-eluting stent to minimize flow disturbance.

## Acknowledgement

This work was supported in part by Short Term Research Exchange Program in summer of year 2005 as well as by Long Term Research Exchange Program in whole of year 2009 of Andong National University.

## References


Berry, J. L., A. Santamarina, J. E. Moore, Jr., S. Roychowdhury and W. D. Routh, 2000, Experimental and computational flow evaluation of coronary stent., *Ann. Biomed. Eng.* **28**, 386-398.

Edelman, E. R. and C. Rogers, 1998, Pathobiologic responses to stenting, *Am. J. Cardiol* **81**, 4E-6E.

LaDisa, John F. Jr., L. E. Olson, I. Guler, D. A. Hettrick, S. H. Audi, J. R. Kersten, D. C. Warltier and P. S. Pagel, 2004, Stent design properties and deployment ratio influence indexes of wall shear stress: A three-dimensional computational fluid dynamics investigation within a normal artery, *J. Appl Physiol.* **97**, 424-430.

Reger, E., G. Sianos and P. W. Serruys, 2001, Stent development and local drug delivery. british medical bulletin **59**, 227-248.

Garasic, J. M., E. R. Edelman, J. C. Squire, P. Seifert, M. S. Williams and C. Rogers, 2000, Stent and artery geometry determine intimal thickening independent of arterial injury, *Circulation* **101**, 812-818.

Bennett, M. R., 2003, In-stent stenosis: pathology and implications for the development of drug eluting stents, *Heart* **89**, 218-224.

Morice, M-C., P. W. Serruys, J. E. Sousa, J. Fajadet, E. B. Hayashi, M. Perin, A. Colombo, G. Schuler, P. Barragan, G. Guagliumi, F. Molnar and R. Falotico, 2002, A randomized comparison of a sirolimus-eluting stent with a standard stent for coronary revascularization, *N. Engl. J. Med.* **346**, 1773-1780.

Moses, J. W., M. B. Leon, J. J. Popma, P. J. Fitzgerald, D. R. Holmes, C. O' Shaughnessy, R. P. Caputo, D. J. Keriakes, D. O. Williams, P. S. Teirstein, J. L. Jaeger and R. E. Kuntz, 2003, Sirolimus-eluting stents versus standard stents in patients with stenosis in a native coronary artery, *N. Engl. J. Med.* **349**, 1315-1323.

Chong, P. H. and J. W. M. Cheng, 2004a, Early experiences and clinical implications of drug-eluting stents: Part 1, *The annals of pharmacotherapy* **38**, 661-669.

Chong, P. H. and J. W. M. Cheng, 2004b, Early experiences and clinical implications of drug-eluting stents: Part 2, *The Annals of Pharmacotherapy* **38** 845-852.

Suzuki, T., G. Kopia, S. Hayashi and L. R. Bailey, 2001, Stent-based delivery of sirolimus reduces neointimal formation in a porcine coronary model, *Circulation* **104** 1188-1193.

Seo, T. W., L. G. Schachter and A. I. Barakat, 2005, Computational study of fluid mechanical disturbance induced by endovascular stents, *Annals of Biomedical Eng.* **33(4)** 444-456.

Wentzel, J. J., R. Krams, C. H. Schuurbiers, J. A. Oomen, J. Kloet, W. J. van der Giessen, P. W. Serruys and C. J. Slager, 2001, Relationship between neointimal thickness and shear stress after wallstent implantation in human coronary arteries, *Circulation* **103** 1740-1745.

Zunino, P., 2004, Multidimensional pharmacokinetic models applied to the design of drug-eluting stents, *Cardiovascular Engineering: An International J.* **4** 181-191.